Ultrasonically enhanced flux-less bonding with Zn-5Al alloy under ambient condition for high-temperature electronics interconnects

PLEASE CITE THE PUBLISHED VERSION

https://doi.org/10.1016/j.jmapro.2021.10.065

PUBLISHER

Elsevier

VERSION

AM (Accepted Manuscript)

PUBLISHER STATEMENT

This paper was accepted for publication in the journal Journal of Manufacturing Processes and the definitive published version is available at https://doi.org/10.1016/j.jmapro.2021.10.065

Ultrasonically enhanced flux-less bonding with Zn-5Al alloy under ambient condition for high-temperature electronics interconnects

Canyu Liu[a], Allan Liu[a,b], Yutai Su[c], Yi Chen[a], Zhaoxia Zhou[d], Changqing Liu[a,*]

[a] *Wolfson School of Mechanical, Electrical and Manufacturing Engineering, Loughborough University, Leicestershire, UK*

[b] *Department of Mechanical Engineering, The University of Sheffield, Western Bank, Sheffield City Centre, UK*

[c] *School of Mechanics, Civil Engineering and Architecture, Northwestern Polytechnical University, Xi'an, P. R. China*

[d] *Loughborough Materials Characterization Center, Loughborough University, Leicestershire, UK*

Abstract

Zn-5Al eutectic alloy is a promising Pb-free solder suitable for high-temperature electronics packaging. However, the soldering with Zn-5Al alloy is undermined by its poor oxidation resistance and wettability in ambient atmosphere, which also demands significant time to complete if transient liquid phase soldering (TLPS) is required. In this work, the TLPS assisted by ultrasonic vibration (USV) under ambient condition without flux has been performed to enhance and accelerate interfacial reactions between Zn-5Al and Cu or Ni substrate. It has been found that the resultant full intermetallic compounds (IMCs) joints with uniform microstructure can be formed within 1 min and 3 min on Cu and Ni substrate, respectively, without flux or protective inert gases. The IMCs resulted from the interfacial reactions have been identified after the completion of TLPS process. For the ultrasonic-assisted TLPS (U-TLPS) of Zn-5Al onto Cu substrate, the joints consist of three IMC layers, CuZn, Cu_5Zn_8, and CuZn with the residual oxide fragments remained at the central line inside of IMC Cu_5Zn_8, where Al is rich likely due to the segregation of element Al during the TLPS process. For the U-TLPS of Zn-5Al onto Ni substrate, three IMC layers, Ni_5Zn_{21}, NiAl and Ni_5Zn_{21} IMC were also observed, with the porous Ni_5Zn_{21} IMC layers present in adjacent to the Ni substrate. Both residual oxide fragments in the Zn-5Al/Cu joints and porous Ni_5Zn_{21} IMC in the Zn-5Al/Ni joints could potentially deteriorate mechanical integrity of the joints, which is yet to be understood.

Key words: Ultrasound-assisted soldering; Transient liquid phase soldering; Zn-5Al solder; High-temperature electronics packaging

1. Introduction

In the packaging and integration of power electronics, conventional Si devices are expected to be replaced by wide-bandgap (WBG) semiconductors (e.g., SiC and GaN), which have the advantages of higher withstanding voltages, operating temperatures and switching frequencies [1]. To exploit the full potentials of the WBG devices, it presents a significant challenge to meet the requirements of interconnects (e.g., die-attach), such as increased operation temperatures, which is likely to exceed 250°C. The assembly through bonding or soldering of wide range of components such as die, substrate to ensure reliable functional performance under such harsh environment is critically important [2].

Currently, high-Pb (>85 Wt% Pb) solders are the most common materials applied in high-temperature electronics packaging because of their suitable melting point range (300 °C – 314 °C) and proven reliability. However, the application of high-Pb solders is under the pressure and likely to be banned by legislations in the future due to the health and environmental concerns [3]. Several Pb-free candidates as the replacements of high-Pb solders have been proposed as high-temperature interconnection materials, including Au-based, Zn-based and nano Ag paste materials [4-5]. Among these, Zn-based solders are of great interests because they are cost-effective and possess excellent thermal and electrical conductivities which well suit the application of high temperature application [6]. The Zn–5 Wt% Al solder alloy at its eutectic point of 381°C is an ideal melting point which in the range of temperature for high temperature electronics applications [7]. However, the main disadvantage of Zn-based solders is their poor oxidation resistance, which undermines their wetting abilities on metal substrates and potentially deteriorates performance and reliability of the formed joints [8]. Conventionally, the flux can improve solderability by removing oxide layer on the surface of metal substrate [9]. However, the compositions of flux are usually complex and less satisfactory, thus limited given the high soldering temperature, and currently, no commercial flux for Zn-Al solder is available in market [10]. The flux for Zn-5Al solder should be active above 400°C, which is much higher than the fluxes designed for Sn-based Pb-free solders (below 250° C). In addition, the flux residues are a main reason of joint failures, which requires extra clean procedures which also presents a significant effort for industry [11]. Many researchers have attempted the vacuum soldering or soldering with protection of inert atmospheres to avoid oxidation [12], but this will add some significant constraints to the applications in the industry, thus less attractive. It is therefore desirable to simplify soldering process by soldering in the ambient condition without flux.

Ultrasonic vibration can supply additional energy inputs to the interfacial bonding due to the friction between the components, which has been applied to welding metals from Second World War in Germany. It can make the joints between two metal parts under lower processing temperature (~50% of metal's melting point) [13]. Recently, there has been growing interests in ultrasonic-assisted soldering [14-15], which has demonstrated the advantages of the ultrasonic energy inputs. Most studies in this field have focused on the current common Sn-based solders [16-17]. It is the cavitation erosion effect of ultrasonic vibration that can break the oxide layers on metal substrate surfaces [18]. Such acoustic steaming and microjets created by cavitation bubbles can enhance the interfacial interaction between solder and substrate [19], which is anticipated to improve the poor wetting ability of Zn-5Al solder.

It has previously been observed that ultrasonic vibration during bonding can enhance the solderability of Zn-14Al (under 35 kHz frequency and 170 W power) [20] and Zn-3Al (under 28.8 kHz frequency and 270 W power) [21]. Wu et al. [22] used Zn-5Al solder to bond SiC ceramics with the assistance of ultrasonic vibration under 20 kHz frequency and 300 W power, which took the advantage of its lower eutectic melting point. Transient liquid phase soldering (TLPS) can be used to form a full IMC joint with higher melting point between melted solder and metal substrate at a lower processing temperature [23]. However, TLPS process can be quite time-consuming (usually > 100 min) as it depends on dependence on the liquid-solid inter-diffusion. It is recognised that TLPS process can be accelerated by ultrasonic vibration. Ultrasound-assisted transient liquid phase soldering (U-TLPS) has been employed as a promising brazing process [24-25]; it has been applied by several researchers for ultrasonic-assisted soldering process with Zn-based alloys [20-22], but none has attempted to apply ultrasonic vibration for TLPS process, which can also be beneficial.

In this study, the interfacial reactions between Zn-5Al and Cu or Ni substrate until full-IMC structures formed by U-TLPS are investigated, where Cu is chosen as the most common substrate widely used in electronics packaging, and Ni coating of several micrometres is often applied as a metallisation, for instance, on the direct bonded copper (DBC), to suppress the excessive growth of interfacial IMCs. The specific objective of this study is to achieve Zn-5Al bonding without flux under ambient atmosphere. Furthermore, the interfacial reactions, IMC formation mechanisms and mechanical properties of these joints were analysed and discussed.

2. Experimental procedures

2.1. Materials and ultrasonic-assisted bonding

The Zn-5 Wt%Al eutectic solder alloy used in this study was supplied by Brock Metal Company, which was produced through casting of proportional high purity Zn (99.9%) and Al (99.9%) metals under protective atmosphere. In our bonding experiments, the Zn-5 Wt%Al eutectic alloy was cold-rolled into sheets of ~80 μm thick followed by dicing them into 5 mm × 5 mm square coupons. The 1 mm thick Cu and Ni sheets (99.9 % purity) supplied by Advent company were also cut into 5 mm × 5 mm square coupons as substrates for bonding process. All the surfaces of metal substrates were polished using sandpapers of 240, 400, 800 and 1200 mesh. Before bonding, an etching process was conducted to remove the oxide layer.

A graphical illustration of the ultrasonic-assisted soldering process is shown in Fig. 1(a). The vertical ultrasonic vibration was induced by an ultrasonic horn on the top of the upper Cu or Ni substrates. The ultrasonic equipment for bonding was supplied by Beijing Ultrasonic Co., Ltd. The weight of ultrasonic horn was around 1.0 kg, which equated a pressure of 0.4 MPa. The vibration frequency was fixed at 20.0 kHz and the power was set as 10 W. As shown in Fig. 1(b), the thermal properties of Zn-5Al solder were analysed by differential scanning calorimetry (DSC). After a eutectoid transformation at 287.1 °C, Zn-5Al solder began to melt from 381.9 °C and completely molten at 388.5 °C. The corresponding reaction heat was 111.9 J/g during melting. The sandwich stacks of the Cu/Zn-5Al/Cu or Ni/Zn-5Al/Ni structures were placed on a hot stage for heating. The peak temperature during bonding was set as 420 °C to ensure solder can be transferred into liquid. The designed thermal profile of U-TLPS process is shown in Fig. 1(c). After heating the samples to 420 °C, ultrasonic vibration was applied for a certain period, and then cooling in ambient atmosphere until room temperature. With the ultrasonic vibration time increasing, the Zn-5Al solder began to react with metal substrate until been fully consumed. As for a comparison, the same Cu/Zn-5Al/Cu or Ni/Zn-5Al/Ni structures were heated without ultrasonic vibration under a pressure of 0.4 MPa, which have the similar heating and cooling process.

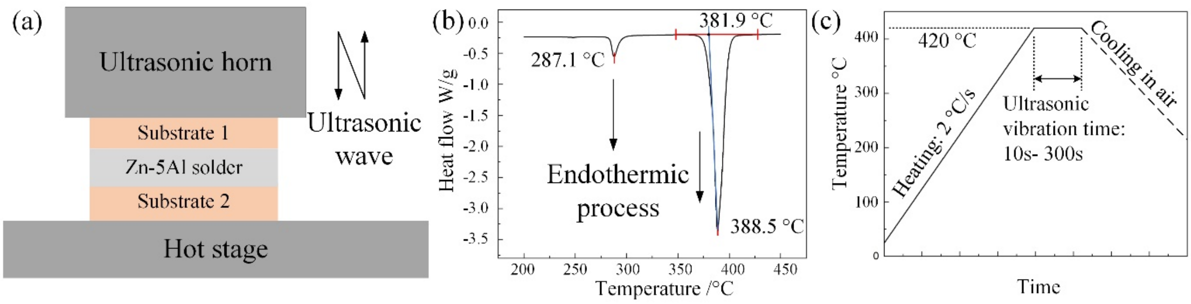

Fig. 1. (a) Schematic of ultrasonic-assisted soldering process, (b) DSC curve of Zn-5Al solder sheet and (c) designed temperature profile during U-TLPS.

2.2. Analysis methods

To observe the cross-section microstructures of joints, the bonded samples were cold mounted and then grounded by 240, 400, 800 and 1200 sandpapers. After the auto polish (Struers, Tegramin) by 9, 3 and 1 μm diamond pastes, the microstructures of soldered Cu/Zn-5Al/Cu and Ni/Zn-5Al/Ni joints was characterized by scanning electron microscopy (SEM, Jeol 7100) and optical microscope (OM, Leica DMi8). The element composition was then analysed by energy dispersive spectroscopy (EDS). A shear test was conducted to evaluate the mechanical properties of bonded joints. The fractured surfaces after shear test were examined by X-ray diffraction (XRD, Bruker D2 phaser) with a scanning step of 0.02°.

3. Results

3.1. Interfacial reactions between Zn-5Al solder and Cu or Ni substrate without ultrasonic vibration assistance

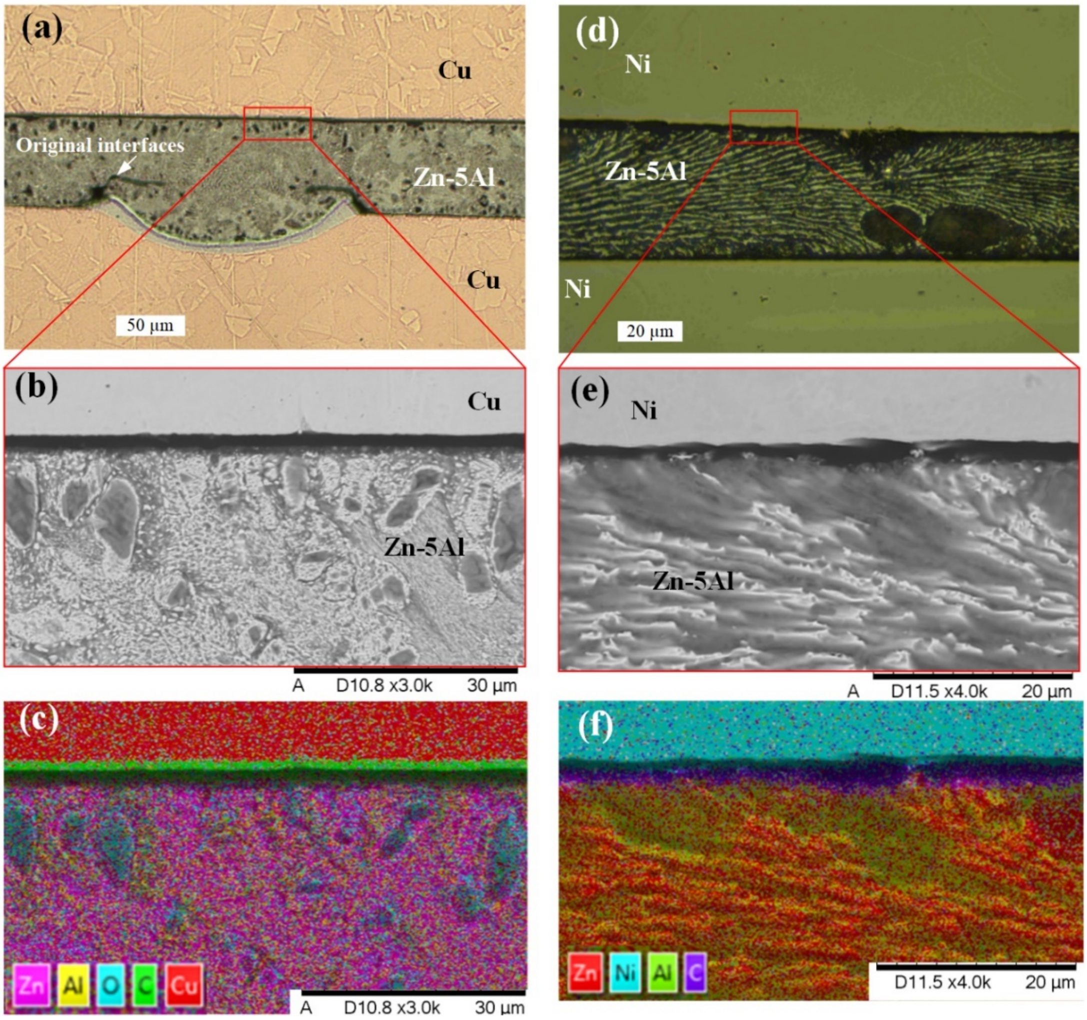

Fig. 2. Cross-section of (a-c) Cu/Zn-5Al/Cu and (d-f) Ni/Zn-5Al/Ni interfaces heated at 420 °C for 300 s without ultrasonic vibration.

Fig. 2 exhibits the cross-section microstructures of Cu/Zn-5Al/Cu and Ni/Zn-5Al/Ni joints without ultrasonic vibration. These joints were heated at the temperature of 420 °C for 300 s under the pressure of 0.4 MPa in ambient atmosphere. Due to the oxidation of Zn-5Al, there was a stable oxide layer on the surface of Zn-Al solder, which resulted in its poor wettability on metal substrate [26]. As shown in Fig. 2(a) and Fig. 2(d), Cu substrate reacted with Zn-5Al solder at some local areas, but no obvious reaction can be found with Ni. The Zn-Al solder is more likely to react with Cu at the Cu/Zn-Al interface compared to Ni substrate. This result shows a good agreement with the previous research, which demonstrated that the IMCs growth rate of Ni/Zn-Al system is much slower than that of Cu/Zn-Al system [12]. In the reacted area, Cu substrate dissolved into liquid Zn-5Al solder and formed an arc shape of local IMC layer. In the meantime, the original solder/substrate interfaces were pushed and lodged into the solder joint. On the contrast, there was no obvious reaction between Zn-5Al solder and Ni substrate, as shown in Fig. 2(d). However, overall, a large unboned area of interface is dominated due to the presence of intrinsic oxide layers, which has been confirmed by SEM results with EDX elemental mappings provided in Fig. 2(b), 2(c) and Fig. 2(e), 2(f) for Cu/Zn-Al and Ni/Zn-Al, respectively.

3.2. Cu/Zn-5Al/Cu bonding assisted by U-TLPS

Ultrasonic vibration has exerted a significant influence on the interfacial reaction of Cu/Zn-5Al/Cu joint. The cross-section microstructures of Cu/Zn-5Al/Cu joints after ultrasonic vibration for 60 s are shown in Fig. 3. The microstructures were investigated by both optical microscope (Fig. 3(a)) and SEM (Fig. 3(b)) to provide more details. As shown in Fig. 3(a), the original Zn-5Al phase patten was disappeared after 60 s of vibration. It indicates that all the Zn-5Al solders have been consumed and the TLPS process was completed, where the oxide layers have been effectively disrupted by ultrasonic vibration. The chemical compositions of resultant IMCs were investigated by EDS and listed in Table 1. The thin IMC layer near Cu substrate was identified as CuZn (*β'*, B2, ordered bcc) and the brighter area in the bulk joint was Cu_5Zn_8 (*γ*, $D8_2$) according to EDS results and Cu-Zn phase diagram [27]. The distribution of Cu and Zn were consistent, as exhibited in Fig. 3(c) and 3(e). However, the traces of fragments were found along the central line of the bonded structure (the discontinued dark regions) enclosed within the bulk layer of Cu_5Zn_8 IMCs.

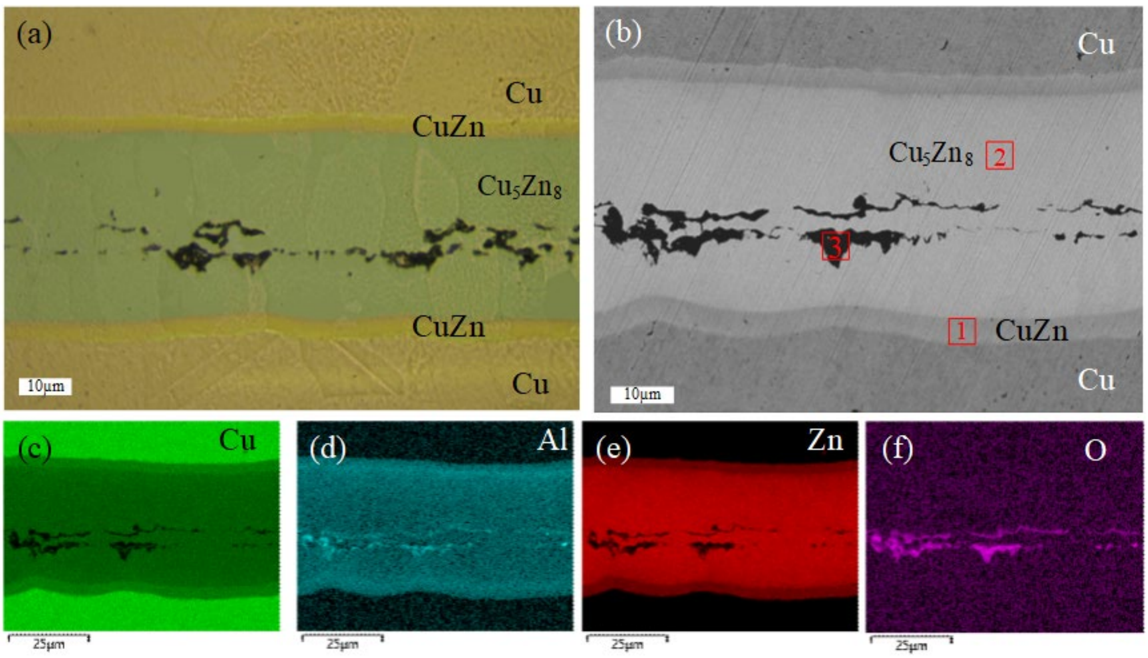

Fig. 3. (a) Optical and (b) SEM image of Cu/Zn-5Al/Cu joints by U-TLPS for 60s, (c-f) EDS elemental mapping images of Cu, Al, Zn and O.

The EDS maps in Fig. 3(c-f) have revealed the dark fragments in the bulk joint shown in Fig. 3(a) and 3(b) are enriched with Al and O elements, but lack of presence of Cu and Zn elements. It can be deduced that these fragments are predominantly the aluminium oxide residuals resulted from the Cu-Zn5Al reactions, and they were subsequently pushed into the middle of the joint due to the ultrasonic vibration. However, it has been noticed that a relatively large amount of Cu and Zn have been detected in these dark region 3 from EDS results in table 1, primarily due to the limited area of the site that EDS probe can accurately focus for inspection. These Zn and Cu are likely attributed from the surrounding Cu_5Zn_8 IMC.

As shown in Fig. 3(d), Al element was not only enriched in the dark fragments areas, but also dispersed in the entire Cu-Zn IMC joint. Given the small amount (5wt%) of Al in the Zn-Al alloy in the solid solution, it is reasonable to assume that Al participated in the interfacial reactions between Zn and Cu, hence the co-existence of Al traces in the Cu-Zn IMCs formed from the reactions. A relative Al-rich CuZn layer has also been observed at the Cu/Zn-Al interfaces where the CuZn phase has a high Cu content compared to Cu_5Zn_8 IMC main body of the joint. This indicates the possible formation of small amount unstable Cu-Al IMCs (e.g. Al_4Cu_9) as reported elsewhere [31] due to the higher affinity of Al to Cu compared with Zn, but they are likely to be dissolved or combined with Cu-Zn IMCs.

Table 1. Element and predicted phase compositions in the regions marked in Fig. 3(b).

Sample	Region	Composition (at %)			Predicted phase
		Cu	Zn	Al	
Cu/Zn-5Al/Cu, 60s	1	51.31	44.20	4.48	CuZn
	2	36.54	60.98	2.48	Cu_5Zn_8
	3	30.74	42.09	27.18	Aluminium-oxide

3.3. Ni/Zn-5Al/Ni bonding assisted by U-TLPS

Compared to Cu/Zn-5Al/Cu joint, longer time was required to form full-IMCs structure in Ni/Zn-5Al/Ni joint. It is well known that the thickness of IMC layer follows the parabolic growth law [33]:

$$h = h_0 + \sqrt{Dt} \quad (1)$$

where h_0 is the thickness of existed IMC layer, D is the diffusion coefficient between elements that forming IMCs, and t is the reaction time. Therefore, it can be concluded that $D_{Ni5Zn21}$ has lower value than D_{Cu5Zn8}. It is similar with the previous study that D_{Ni3Sn4} smaller than D_{Cu5Sn6} [12]. In addition, the diffusion coefficient D is determined by Arrhenius relationship [33]:

$$D = D_0 e^{-Q/RT} \quad (2)$$

where D_0 is a pre-exponential frequency factor, R is the gas constant, T is the absolute temperature and Q is the activation energy. Therefore, the diffusion coefficient D will be increased when the activation energy Q decreased. Ultrasonic vibration is expected to increase the vibration amplitude of Cu and Ni atom, which can reduce the activation energy Q and then promote the IMCs growth rates [34]. The cross-sections of Ni/Zn-5Al/Ni joints after ultrasonic-assisted bonding for 180 s are shown in Fig. 4. The bright layers near both substrate/solder interfaces contained more Zn and Ni element, which were identified as Ni_5Zn_{21} (γ, $D8_2$) according to EDS results (Table 2) based on the Ni-Zn phase diagram [12]. Al-rich phases were found to primarily distribute around the central line of the joint (Fig. 5(a)), no Al content was detected near substrate/solder interfaces. It is also interesting to observe the higher counts of the Ni and O elements around the central line of the joint (Fig. 4(c) and 4(f)), but less Zn in this region (Fig. 4(d)). Based on the EDS results and Ni-Al phase diagram the Al- and Ni- enriched phases around the central line are likely consist of NiAl (B2, ordered bcc) [12].

As marked in Fig. 4(a), clearly, a highly compact Ni_5Zn_{21} layer near Ni substrate was formed, but it has appeared that this was accompanied with numerous evenly distributed micro-voids in the transition zone between the Ni_5Zn_{21} layer and the NiAl phase around the central line. The similar porous structure with Ni_5Zn_{21} phase was also reported as the results of the liquid-solid state interfacial interactions in the Zn-20 wt.%Sn/Ni system [30]. However, the formation mechanism of such a composite joint is yet to be explained in detail. The volume shrinkage due to the formation of IMCs is commonly accepted to explain formation of voids. Sun et al. [35] investigated the porous structure formed during Cu-Sn TLPS process, giving an estimation of 4.38 % volume reduction when Cu_6Sn_5 was transformed into Cu_3Sn. Xu et al. [36] observed the void growth during Au-Al wire bonding and calculated the volume shrinkage based on the changes of molar volumes of phases using the formula as follows [36]:

$$V_m = V_c N_A / Z \quad (3)$$

Where V_m is the molar volume, V_c is the unit cell volume, N_A is the Avogadro constant (6.022×10^{-23}/mol) and Z is the number of formula units per unit cell. The molar volumes of Ni, Zn and Ni_5Zn_{21} were shown in Table 3. It can be calculated that the volume shrinkage was 3.31% when Ni_5Zn_{21} was formed. Therefore, the volume shrink mechanism should be responsible for the voids formed in Ni_5Zn_{21}, which combined with the growth of IMCs.

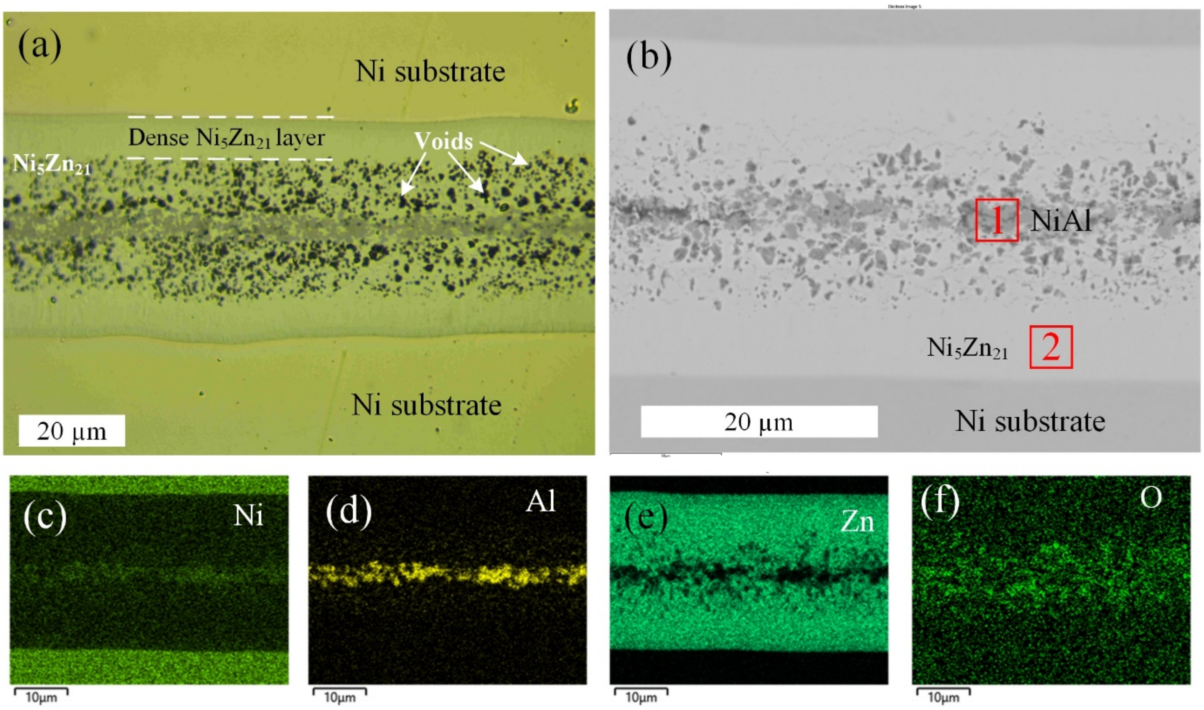

Fig. 4. (a) Optical and (b) SEM images of Ni/Zn-5Al/Ni joints by U-TLPS for 180s, (c)-(f) EDS elemental mapping of Ni, Al, Zn and O, respectively.

Sample	Region	Composition (at %)			Phase
		Ni	Zn	Al	
Ni/Zn-5Al/Ni, 180 s	1	41.73	11.05	47.22	NiAl
	2	19.69	78.80	1.51	Ni_5Zn_{21}

Table 3. Calculated molar volume of Ni, Zn and Ni_5Zn_{21}

Phase	Compound symmetry	Unit cell volume (Å^3)	Number for formular units per unit cell	Molar volume (cm^3 mol^{-1})
Ni	fcc	43.37	4	6.53 [37]
Zn	hcp	88.88	6	8.92 [37]
Ni_5Zn_{21}	Cubic	706.39 [38]	2	212.69

4. Discussion

4.1. Interfacial interactions and IMCs formation during U-TLPS of Zn-5Al on Cu substrate

To investigate the evolution of Zn-5Al/Cu interfacial reactions during U-TLPS, the bonding with an ultrasonic vibration time of 10 s was conducted. As shown in Fig. 5, after the ultrasonic vibration of 10 s, the TLPS process was not completed and residual unreacted Zn-5Al solders were remaining. According to the EDS results (Table 4) and Zn-Cu phase diagram [12], three IMC layers were found after the liquid Zn-Al-Cu solid interfacial reaction. A thin layer of CuZn (*β'*, B2, ordered bcc) formed in direct contact with the Cu substrate, followed by a thick compact Cu_5Zn_8 (*γ*, $D8_2$) layer formed in the middle and a number of 'scallop-shape' $CuZn_5$ 'islands' away from the interface inside the solder. Clearly, from the metallurgical perspectives where the interfacial reactions were primarily driven by liquid-solid inter-diffusion, the CuZn with more Cu content emerged in the adjacent to Cu substrate due to easy access to Cu in the substrate. However, the $CuZn_5$ (*ε*, A3, disordered hcp) IMC were formed near the Zn-5Al solder where more Zn were accessible compared to the Cu.

As shown in Fig. 6, XRD was applied to investigate the fractured surface of bonded Cu/Zn-5Al/Cu joints after shear test. Both upper and bottom side have been investigated. The durations of ultrasonic vibration were 60 s and 10 s in Fig. 6(a) and Fig. 6(b), respectively. It can be seen in Fig. 6(a) that phases exposed from the fracture surface were mainly Cu_5Zn_8 and Cu. A small amount of $CuZn_5$ (*ε*, A3, disordered hcp) was also found, which was another potential IMC expected to be formed during Cu-Zn reaction [27]. The upper side and bottom side in Fig. 6(a) contained the same types of IMCs, which indicated that the sample was fractured from the middle of the solder. The average shear strength Cu/Zn-5Al/Cu joints after ultrasonic vibration for 60 s is ~12.73 MPa, which is expected due to the entrapment of fragmented oxides as observed in Fig. 3. It is our main aim to minimise the inclusion of oxides in the joints to form stronger and more harmonised joint structures. According to the XRD results in Fig. 6(b), Cu_5Zn_8, $CuZn_5$, Cu and Zn were all revealed in the upper side of the fracture surface, while only Cu was found in the bottom side. This was consistent with the findings from Fig. 5 that the U-TLPB process was forced to terminate, thus the reaction of Zn-Al solder was incomplete due to a short time (~10 s) of ultrasonic vibration. It can therefore be concluded from the XRD results that the joint through shear test was separated from solder/substrate interface, unlike the one shown in Fig. 6(a).

Although Zn-5Al solder alloy contains 5 Wt % aluminium, only Cu-Zn IMCs were identified after U-TLPS process. The Al_2Cu as a typical IMC can be formed during Al/Cu liquid/solid diffusion [42], but it was not found in this study. Similar observations were also reported in prior studies that related to Zn based alloy/Cu interfacial reaction [27-29]. Yoshikazu et al. [27] investigated the reaction between Cu substrate with Zn-4Al and Zn-4Al-1Cu solders in Ar atmosphere and found that $CuZn/Cu_5Zn_8/CuZn_5$ three layers were formed at the interface for both Zn-4Al and Zn-4Al-1Cu solders. They also observed the Al distributed in the Cu-Zn IMC layers with varying concentrations, nevertheless, no Cu-Al IMCs were detected. The similar findings were also reported when using Zn-4Al-6Ag [29] and Zn-Al-Mg-Ga [28] solder alloys for soldering onto Cu substrate. A possible explanation might be the higher reactivities of Al compared to Zn, which was more prone to react with O in the air. Because of small amount Al in the alloy, it can be quickly consumed before they are able to react with Cu. Also, Zn would preferentially react with Cu, then pushed Al or Al_2O_3 and make them segregated in the central areas.

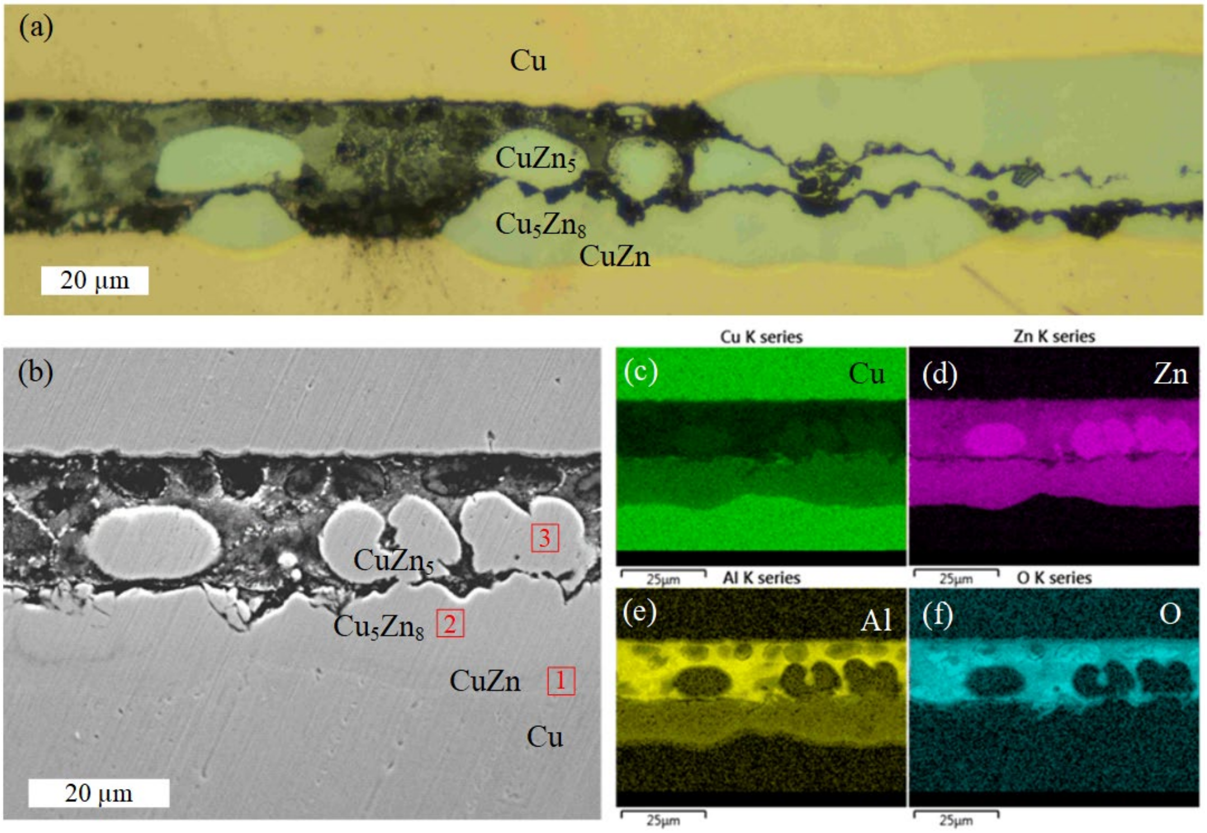

Fig. 5. (a) Optical, (b) SEM and (c-f) EDS images of Cu/Zn-5Al/Cu joints interface after ultrasonic-assisted soldering for 10s.

Table 4. Elemental analysis and identified phases of the marked locations in Fig. 5(b).

Sample	Region	Composition (at %)			Predicted phase
		Cu	Zn	Al	
Cu, 10s	1	43.64	46.60	9.77	CuZn
	2	34.70	58.06	7.24	Cu_5Zn_8
	3	21.15	73.23	5.63	$CuZn_5$

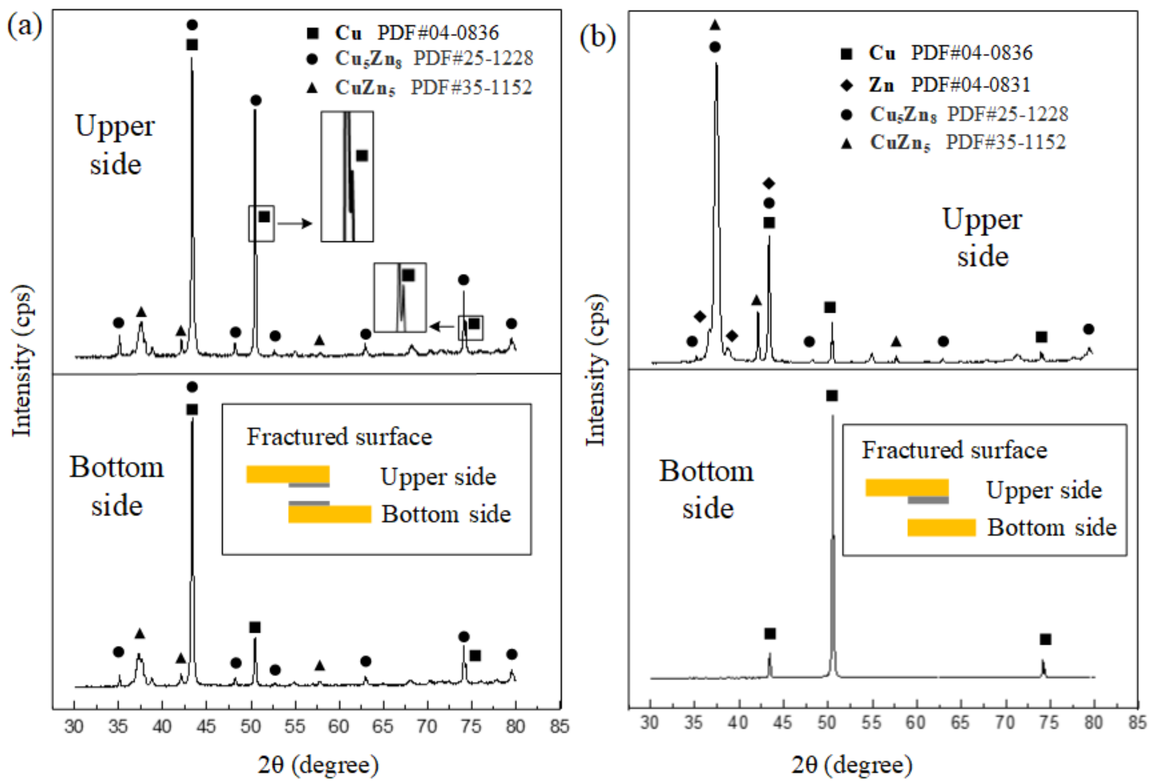

Fig. 6. XRD results of fractured Cu/Zn-5Al/Cu joints after ultrasonic vibration of (a) 60s and (b) 10s.

According to our experimental results, the mechanism of Cu/Zn-5Al/Cu interfacial reaction assisted by U-TLPS can be proposed as schematically shown in Fig. 7(a). It can include 3 connected consecutive stages until the full-IMCs bond structure to be formed as the time of ultrasonic vibration increases. At the initial stage, as shown in Fig. 7(a), the cavitation bubbles induced by acoustic vibration in liquid solder are constantly transmitting impinging the Cu substrate surface with high speed [19]. Such cavitation erosion can effectively break solid oxidation layers on both solder and Cu substrate [18]. The next stage began with the penetration of the liquid solder into the broken oxide layers followed by an instant interfacial reaction between solder and Cu, as soon as the oxide barriers are ineffective, where the exposure and direct contact between fresh Cu surface and Zn-5Al solder can occur. This led to CuZn/Cu_5Zn_8/$CuZn_5$ IMC layers formed, with $CuZn_5$ being discontinuous at the liquid/solid interface, but gradually transformed into Cu_5Zn_8, as Zn-5Al solders are completely consumed with the vibration time. The final joints only consist of the CuZn IMC immediately in adjacent to Cu substrate but connected to the bulk Cu_5Zn_8 IMC as the main body of the interconnect. Given the high stability of Al_2O_3 that may be formed due to extremely high affiliation nature of Al with O_2 in the ambient air, the only small amount Al is likely to be converted into its oxide with the least chance of being involved in the formation of Zn-Cu IMCs during U-TLPS process. Consequently, such formed fragmented Al_2O_3 flakes are flushed in the liquid solder and eventually pushed and migrated from both side of the Cu/Zn-5Al interfaces into the region of central line of the final joint. The existence of Al_2O_3 flakes can potentially weaken the joint, which otherwise can very strong because of the full IMCs formed in the joint.

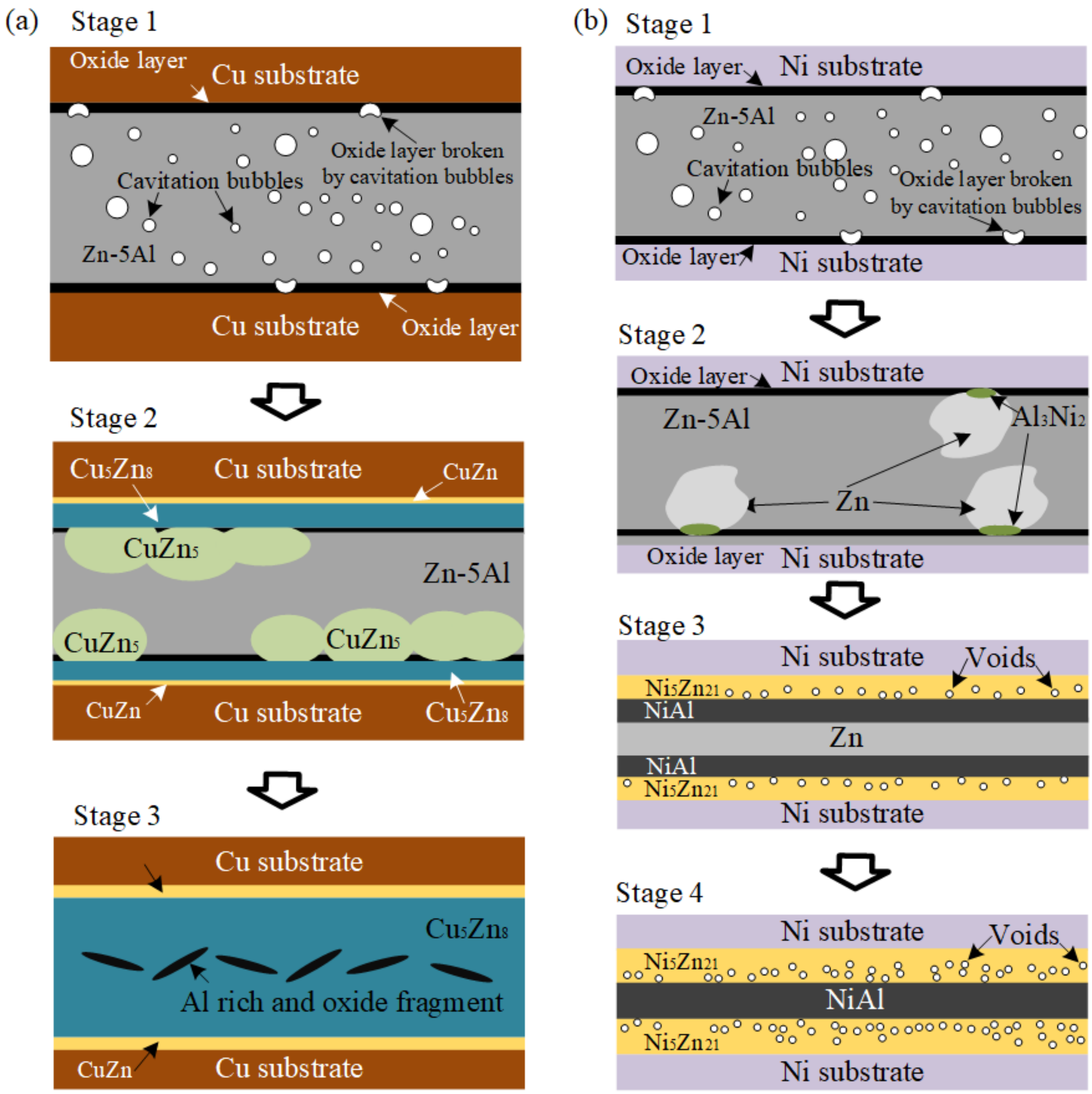

Fig. 7. Schematics of (a) Cu/Zn-5Al/Cu and (b) Ni/Zn-5Al/Ni interfacial reaction and mechanism of IMC formation during U-TLPS.

4.2. Interfacial interactions and IMCs formation during U-TLPS of Zn-5Al on Ni substrate

Cross-sectional micrographs of a Zn-5Al/Ni joint and the enlarged interface formed by U-TLPS process under the ultrasonic vibration of 10 s are shown in Fig. 8(a) and 8(b), with the elemental EDS maps provided in Fig. 8(a’) and 8(b’), respectively. The determination of phase composite through EDS analysis in Table 5 clearly shows the formation of Al_3Ni_2 IMCs at the interface between Zn-5Al solder and Ni substrate. However, whilst the eutectic structure of Zn-5Al solder in the central part remained unchanged, there are several 'egg-shaped' Zn-rich non-eutectic patches emerged near the interfaces from the EDS results in Table 5. It is reasonable to assume that the Al element was primarily segregated from the initial Zn-5Al solder, then migrated towards to and reacted with Ni substrate, which had left behind several patches of Zn-rich phases. From Fig. 8(c) where the ultrasonic vibration time increased to 60 s, the original Zn-5Al solder alloys had completely reacted with the Ni substrate with no eutectic microstructure of Zn-5Al observable. EDS results from the region 3 in Fig. 8(c) given in Table 5 confirmed that there was no Al element remained in the middle area of the joint, indicating the completely depletion of Al in Zn-5Al alloy due to primarily the interfacial reactions with Ni substrate. Interestingly, the vibration time of 60 s had been sufficient for the interfacial reactions between Zn and Ni, which has resulted the formation of IMC Ni_5Zn_{21} at the interfaces as evidenced by EDS analysis in Table 5 of the region 5 in Fig. 8(c). However, a large amount of Zn were unable to react with Ni and converted into Ni_5Zn_{21}. After Al had been all consumed by Ni, the remaining reaction can only occur between the liquid Zn and Ni. Eventually, Zn in the middle area may diffuse thru the Al-Ni IMCs to react with Ni substrate to form a complete Zn-Ni IMC joint.

Based on the above experimental findings, four stages of Ni/Zn-5Al/Ni interfacial reactions during U-TLPS process can be proposed as schematically illustrated in Fig. 7(b). In Stage 1, the ultrasonic cavitation bubbles began to impinge and break the oxide layers on Ni surface at numerous sites. The active Al atoms in the liquid Zn-Al solder can then preferentially react with Ni, which consequently leads to the Stage 2 where the Ni-Al interfacial reactions and the formation of IMC Al_3Ni_2 inevitably result in the several patches of Zn-rich phases near the interfaces due to the break-up of the initial eutectic Zn-5Al microstructure. At Stage 3, the depletion of most Al in the solder makes it possible for plenty remaining Zn to react with Ni to form Ni_5Zn_{21}. In this Stage 3 the diffusion or transportation of Zn through the suitable paths in the Al-Ni IMCs is necessary to reach and react with Ni, hence the Al-Ni IMCs can be pushed inward to allow the growth of Zn-Ni IMCs at the solder/Ni interface. Finally, at Stage 4, while the Ni_5Zn_{21} IMC layer is gradually transformed into Al_3Ni_2 then the final stable IMC AlNi as Zn-Ni reaction extends, thus a final full IMCs composite joint consisting of Ni_5Zn_{21}/NiAl/Ni_5Zn_{21} triple layers is anticipated with sufficient U-TLPS time to allow the remaining Zn to be fully converted into its IMCs.

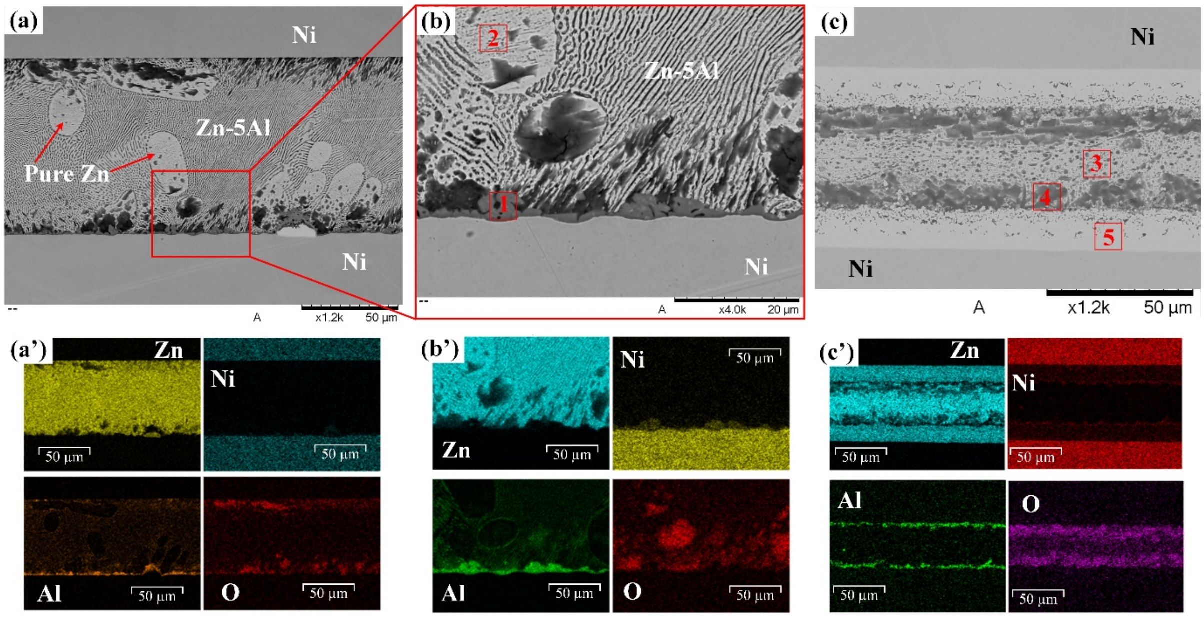

Fig. 8. SEM and EDS images of Ni/Zn-5Al/Ni joints interface after ultrasonic-assisted soldering for (a, b) 10s and (c) 60s.

When comparing the interfacial reaction between Zn-5Al/Ni and Zn-5Al/Cu liquid/solid diffusion, the most remarkable difference was the behaviour of Al. No obvious Cu-Al IMCs formed during the whole U-TLPS process, which has been exhibited by the current research and previous publications [27-29]. On the contrary, Al_3Ni_2 was detected before the forming of Cu-Zn IMCs, which was also demonstrated by the current results and prior studies [12, 28]. Yoshikazu et al. [12] analysed the solderability of Zn-Al(-Cu) eutectic alloys on Ni substrate. Only Al_3Ni_2 formed in the interface with a soldering temperature of 420 °C. When the temperature increased to 450 °C, Al_3Ni_2 was firstly appear and then Ni_5Zn_{21} IMC layer was detected. In the current study, Ni_5Zn_{21} was formed even through the temperature was only 420 °C. It can be explained by the cavitation effect of ultrasonic vibration, which can produce high instantaneous temperature in liquid solder [19]. Haque et al. [28] utilised Zn-Al-Mg-Ga solder to attach Si die on Cu substrate. There was a Ti/Ni/Ag metallization on the back of Si die. Since the 200 nm Ag layer was easily dissolved during soldering, Zn-Al-Mg-Ga solder got the chance to react with Ni layer. However, only Al_3Ni_2 IMC was found on the die side. Although this phenomenon has been found, the forming mechanism is yet to be understood. A possible explanation might be the difference of valency. According to the Hume-Rothery rules [32], a kind of metal with a lower valency is more likely to dissolve in another kind of metal which has a higher valency. Both Ni and Zn have the valence of 2, but Al has the valence of 3. Therefore, Ni is more likely dissolved in Al rather than Zn. On the other hand, Cu has the valence of 1, which means it can be dissolved in both Zn and Al. The relatively low concentration and oxidation issue may limit the reaction between Al and Cu.

Table 5. Element and possible phase compositions marked in Fig. 8.

Sample	Region	Composition (at %)			Predicted phase
		Ni	Zn	Al	
Ni/Zn-5Al/Ni, 10s	1	38.37	3.71	58.92	Al_3Ni_2
	2	1.33	97.25	1.46	Zn
Ni/Zn-5Al/Ni, 60s	3	1.25	95.31	3.44	Zn
	4	42.23	5.48	52.29	NiAl or Al_3Ni_2
	5	20.32	78.80	0.89	Ni_5Zn_{21}

5. Conclusion

In this comparative study, the formation of the solder joints Cu/Zn-5Al/Cu and Ni/Zn-5Al/Ni has been successfully achieved by soldering Zn-5Al eutectic alloys onto both Cu and Ni substrates assisted by U-TLPS under the ambient condition without uses of flux. The interfacial reactions and mechanisms of IMCs between solder and metal substrates were examined in detail to understand the underlying fundamental mechanisms, and the main conclusions are summarized as follows:

(1) Compared to the conventional thermal-compression bonding, ultrasonic vibration applied in U-TLPS process enhances the solderability of Zn-5Al alloy through: i) promoting the interfacial reaction by breaking down the oxide layers of the surfaces, and ii) accelerating the liquid-solid reaction by increasing the diffusion effectiveness.

(2) Using the developed U-TLPS process, the formation of complete full-IMC joint structures can be significantly accelerated; it only takes ~1 min and ~3 min to complete the reaction to form full IMC joints between Cu and Zn-5Al, and between Ni and Zn-5Al, respectively. The typical IMC layered structures induced by U-TLPS process for bonding with Cu and Ni with Zn-5Al alloy are CuZn/Cu_5Zn_8/CuZn, and Ni_5Zn_{21}/NiAl/Ni_5Zn_{21}, respectively.

(3) For U-TLPS bonding Cu with Zn-5Al alloy, the interfacial reaction begins from the formation of β'-CuZn, γ- Cu_5Zn_8 and ε-$CuZn_5$ layers, where $CuZn_5$ phase is gradually transformed into Cu_5Zn_8 as vibration time increases. Al element in the alloy is hardly involved the interfacial reaction but pushed towards the central line in the form of oxide residuals, which is likely detrimental to the joint mechanical integrity.

(4) For U-TLPS bonding Ni with Zn-5Al alloy, Al element in the solder preferentially reacts with Ni substrate by forming Al_3Ni_2 near the Zn-5Al/Ni interfaces. However, as the bonding progresses the penetration and diffusion of Zn through this Al_3Ni_2 IMC layer led to the formation of the Ni_5Zn_{21} phase between Al_3Ni_2 IMC layer and Ni substrate. As the bonding time increases the growth of the Ni_5Zn_{21} layer can result in the migration of Al_3Ni_2 phase towards the central line, and the Ni_5Zn_{21} layer becomes more porous, which could be responsible for the deterioration of the bonding strength.

(5) In the U-TLPS reaction the affinity of Zn and Al with Cu or Ni substrate which can be described by Hume-Rothery rules indicates that the Al in the solder alloy which has a higher valency is prone to the preferential reaction with Ni, but in Cu bonding, it is the Zn in the alloy that is more susceptible to react with Cu, since Cu can be dissolved in both Zn and Al due to its lowest valence. However, the small amount Al in the solder alloy becomes a limited factor in both cases, hence the reactions with Zn largely occur to form the main body of the Zn-based IMC joints.

Acknowledgements

The authors acknowledge the EPSRC research grants (UK): (i) Underpinning Power Electronics 2017 – Heterogeneous Integration (HI) project (Grant No. EP/R004501/1), and (ii) Quasi-ambient bonding to enable cost-effective high temperature Pb-free solder interconnects (QAB) project (Grant No. EP/R032203/1). The author Canyu Liu would like to acknowledge the studentship of Loughborough University as well as financial support received from the China Scholarship Council (CSC) (Reference No. 201806220073). The authors acknowledge use of facilities within the Loughborough Materials Characterization Centre.

References

[1] Millán, José, et al. "A survey of wide bandgap power semiconductor devices." *IEEE transactions on Power Electronics* 29.5 (2013): 2155-2163.

[2] Zhang, Shuye, et al. "Cu-Cu joining using citrate coated ultra-small nano-silver pastes." *Journal of Manufacturing Processes* 62 (2021): 546-554.

[3] Koga, Shunichi, et al. "Fabrication of Nanoporous Cu Sheet and Application to Bonding for High-Temperature Applications." *Journal of Electronic Materials* 49.3 (2020): 2151-2158.

[4] Yoon, Jeong-Won, et al. "Bonding of power device to ceramic substrate using Sn-coated Cu micro paste for high-temperature applications." *Applied Surface Science* 515 (2020): 146060.

[5] Zhang, Dongxiao, et al. "Preparation and Application of Cu-Ag Composite Preforms for Power Electronic Packaging." *2019 IEEE 69th Electronic Components and Technology Conference (ECTC)*. IEEE, 2019.

[6] Chang, Che-Wei, and Kwang-Lung Lin. "High-Temperature Mechanical Properties of Zn-Based High-Temperature Lead-Free Solders." *Journal of Electronic Materials* 48.1 (2019): 135-141.

[7] Hasan, Mohammad Mehedi, Ahmed Sharif, and M. Abdul Gafur. "Characteristics of eutectic and near-eutectic Zn–Al alloys as high-temperature lead-free solders." *Journal of Materials Science: Materials in Electronics* 31.2 (2020): 1691-1702.

[8] Niu, Xi, and Kwang-Lung Lin. "Effects of Al, Pr additions on the wettability and interfacial reaction of Zn–25Sn solder on Cu substrate." *Journal of Materials Science: Materials in Electronics* 28.1 (2017): 105-113.

[9] Kwon, Soonyong, Hoo-Jeong Lee, and Sehoon Yoo. "Effects of flux formulation temperature on printing and wetting properties of Sn–3.0 Ag–0.5 Cu solder." *Journal of Materials Science: Materials in Electronics* 30.9 (2019): 8493-8501.

[10] Ismail, Norliza, et al. "Effect of flux functional group for solder paste formulation towards soldering quality of SAC305/CNT/Cu." *Soldering & Surface Mount Technology* (2020).

[11] Piotrowska, Kamila, Magdalena Grzelak, and Rajan Ambat. "No-clean solder flux chemistry and temperature effects on humidity-related reliability of electronics." *Journal of Electronic Materials* 48.2 (2019): 1207-1222.

[12] Takaku, Yoshikazu, et al. "Interfacial reaction between Zn-Al-based high-temperature solders and Ni substrate." *Journal of Electronic Materials* 38.1 (2009): 54-60.

[13] Kumar, S., et al. "Application of ultrasonic vibrations in welding and metal processing: a status review." *Journal of Manufacturing Processes* 26 (2017): 295-322.

[14] Xiao, Yong, et al. "Ultrasound-assisted soldering of alumina using Ni-foam reinforced Sn-based composite solders." *Ceramics International* 43.16 (2017): 14314-14320.

[15] C. Liu, A. Liu, Y. Zhong, S. Robertson, Z. Zhou and C. Liu, "Ultrasonic-assisted nano Ag-Al alloy sintering to enable high-temperature electronic interconnections," *2020 IEEE 70th Electronic Components and Technology Conference (ECTC)*, Orlando, FL, USA, 2020, pp. 1999-2004, doi: 10.1109/ECTC32862.2020.00311.

[16] Yi, Xiong, Ruhua Zhang, and Xiaowu Hu. "Study on the microstructure and mechanical property of Cu-foam modified Sn3. 0Ag0. 5Cu solder joints by ultrasonic-assisted soldering." *Journal of Manufacturing Processes* 64 (2021): 508-517.

[17] Hu, Xiaowu, et al. "Effects of ultrasonic treatment on mechanical properties and microstructure evolution of the Cu/SAC305 solder joints." *Journal of Manufacturing Processes* 64 (2021): 648-654.

[18] Wang, Haozhe, et al. "Interfacial morphology evolution of a novel room-temperature ultrasonic bonding method based on nanocone arrays." *Applied Surface Science* 324 (2015): 849-853.

[19] Li, Zhengwei, et al. "Cavitation at filler metal/substrate interface during ultrasonic-assisted soldering. Part I: Cavitation characteristics." *Ultrasonics Sonochemistry* 49 (2018): 249-259.

[20] Ji, Hongjun, Hao Chen, and Mingyu Li. "Overwhelming reaction enhanced by ultrasonics during brazing of alumina to copper in air by Zn-14Al hypereutectic filler." *Ultrasonics Sonochemistry* 35 (2017): 61-71.

[21] Xiao, Yong, et al. "Interfacial reaction behavior and mechanical properties of ultrasonically brazed Cu/Zn–Al/Cu joints." *Materials & Design* 73 (2015): 42-49.

[22] Wu, Bingzhi, et al. "Microstructural evolution of SiC joints soldered using Zn–Al filler metals with the assistance of ultrasound." *Ultrasonics sonochemistry* 44 (2018): 280-287.

[23] Sun, Lei, et al. "Interfacial reaction, shear behavior and microhardness of Cu-Sn TLP bonding joints bearing CuZnAl powder for 3D packaging." *Journal of Manufacturing Processes* 68 (2021): 1672-1682.

[24] Li, Yinan, et al. "Microstructure and Formation Mechanism of Ultrasound-Assisted Transient Liquid Phase Bonded Magnesium Alloys with Ni Interlayer." *Materials* 12.22 (2019): 3732.

[25] Pan, Hao, et al. "Enhancing the solid/liquid interfacial metallurgical reaction of Sn + Cu composite solder by ultrasonic-assisted chip attachment." *Journal of Alloys and Compounds* 784 (2019): 603-610.

[26] Xu, Zhiwu, et al. "Behaviors of oxide film at the ultrasonic aided interaction interface of Zn–Al alloy and Al_2O3p/6061Al composites in air." *Materials Science and Engineering: A* 415.1-2 (2006): 80-86.

[27] Takaku, Yoshikazu, et al. "Interfacial reaction between Cu substrates and Zn-Al base high-temperature Pb-free solders." *Journal of Electronic Materials* 37.3 (2008): 314-323.

[28] Haque, A., et al. "Die attach properties of Zn–Al–Mg–Ga based high-temperature lead-free solder on Cu lead-frame." *Journal of Materials Science: Materials in Electronics* 23.1 (2012): 115-123.

[29] Prach, Michal, and Roman Koleňák. "Soldering of copper with high-temperature Zn-based solders." *Procedia Engineering* 100 (2015): 1370-1375.

[30] Wang, Chao-hong, Hsien-hsin Chen, and Po-yi Li. "Interfacial reactions of high-temperature Zn–Sn solders with Ni substrate." *Materials Chemistry and Physics* 136.2-3 (2012): 325-333.

[31] Gancarz, Tomasz, Janusz Pstruś, and Katarzyna Berent. "Interfacial Reactions of Zn-Al Alloys with Na Addition on Cu Substrate During Spreading Test and After Aging Treatments." *Journal of Materials Engineering and Performance* 25.8 (2016): 3366-3374.

[32] Hume-Rothery, William. "The structure of metals and alloys." *Indian Journal of Physics* 11 (1969): 74-74.

[33] Ghosh, Rituparna, Anwesha Kanjilal, and Praveen Kumar. "Effect of type of thermo-mechanical excursion on growth of interfacial intermetallic compounds in Cu/Sn-Ag-Cu solder joints." *Microelectronics Reliability* 74 (2017): 44-51.

[34] Han, X., Li, X., Yao, P. and Chen, D. (2021), "Influence of ultrasounds on interfacial microstructures of Cu-Sn solder joints", *Soldering & Surface Mount Technology*, Vol. 33 No. 4, pp. 206-214. https://doi.org/10.1108/SSMT-06-2020-0026

[35] Sun, Lei, Ming-he Chen, and Liang Zhang. "Microstructure evolution and grain orientation of IMC in Cu-Sn TLP bonding solder joints." *Journal of Alloys and Compounds* 786 (2019): 677-687.

[36] Xu, H., et al. "New mechanisms of void growth in Au–Al wire bonds: Volumetric shrinkage and intermetallic oxidation." *Scripta Materialia* 65.7 (2011): 642-645.